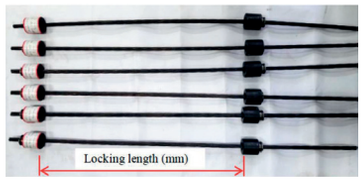
Coupling effect analysis of tension and reverse torque during axial tensile test of anchor cable



Análisis del efecto de acoplamiento de la tensión y del par inverso durante el ensayo de tracción axial de un cable de anclaje

Shuren Wang[1, 2*], Zeliang Wang[1], Jian Gong[1, 2], Yuhao Wang[1], and Qingxiang Huang[3]

[1] School of Civil Engineering, Henan Polytechnic University, Jiaozuo 454003, China
[2] International Joint Research Laboratory of Henan Province for Underground Space Development and Disaster Prevention, Henan Polytechnic University, Jiaozuo 454003, China
[3] College of Engery Engineering, Xi'an University of Science and Technology, Xi'an 710054, China
[*] Corresponding author, e-mail: w_sr88@163.com

DOI: http://dx.doi.org/10.6036/9603 | Recibido: 01/12/2019 • Inicio Evaluación: 12/12/2019 • Aceptado: 17/02/2020

RESUMEN

- En vista de la falta de análisis del efecto de acoplamiento de la tensión y el par inverso de un cable de anclaje, se ha utilizado un equipo de desarrollo propio para realizar un ensayo de tracción en los cables de anclaje de tres diámetros diferentes (9,5 mm, 12,7 mm, 15,2 mm) en condiciones de rotación libre y sin rotación. Posteriormente se construyó el modelo numérico tridimensional del cable de anclaje, se simuló el proceso del ensayo de tensión axial y los resultados computacionales fueron coherentes con los resultados experimentales. Basándose en el principio de trabajo y energía, se propone una fórmula para la fuerza de tracción para el desacoplamiento de la tracción y el par inverso del cable de anclaje. Los resultados muestran que tanto la tensión como el par máximo aumentan con el diámetro del cable de anclaje, y el efecto de la longitud de bloqueo en la tensión y el par máximo no es algo obvio. El cable de anclaje genera un par inverso cuando se tira de él sin rotación, el proceso de cambio de par se divide en las fases elástica y plástica, el par en la fase elástica aumenta linealmente con el aumento de la fuerza de tracción, mientras que el par en la fase plástica permanece estable y la fuerza de tracción aumenta ligeramente. Bajo la condición de rotación libre, el módulo elástico del cable de anclaje disminuirá, el porcentaje de la fuerza de tracción utilizada para desenrollar tres cables de diferentes diámetros (9,5 mm, 12,7 mm, 15,2 mm) fue del 11%, 12% y 10%, respectivamente. Las conclusiones obtenidas en el estudio pueden servir de referencia para orientar prácticas similares en ingeniería.
- **Palabras clave:** Cable de anclaje, Ensayo de tracción, Acoplamiento tensión-torsión, Propiedades mecánicas, Simulación numérica.

ABSTRACT

In view of lack of the coupling effect analysis of tension and reverse torque of the anchor cable, the self-developed equipment was used to perform a tensile test on the anchor cables with three different diameters (9.5 mm, 12.7 mm, 15.2 mm) under free rotation and without rotation conditions. Then the three-dimension numerical model of the anchor cable was built, the process of the axial tension test was simulated and the computational results were consistent with experimental results. Based on the work and energy principle, a formula for the tensile force is proposed for the decoupling tensile and reverse torque of the anchor cable. Results show that the peak tension and peak torque both increase with the diameter of the anchor cable, and the effect of the locking length on the peak tension and torque is not obvious. The anchor cable will generate reverse torque when it is pulled without rotation, the torque change process is divided into the elastic and plastic phases, the torque in the elastic phase increases linearly with the increase of the tensile force, while the torque in the plastic phase remains stable and the tensile force increases slightly. Under the condition of free rotation, the elastic modulus of the anchor cable will decrease, the percentage of the pulling force used for untwisting of three different diameter cables (9.5 mm, 12.7 mm, 15.2 mm) were 11%, 12%, and 10%, respectively. The conclusions obtained in the study can provide a reference to direct the similar engineering practice.

Keywords: Anchor cable, Tensile test, Tension-torsion coupling, Mechanical properties, Numerical simulation.

1. INTRODUCTION

The prestressed anchor cable can give full play to the self-supporting potential of the rock mass, adjust and improve the strength and self-stability of the rock and soil, reduce the self-weight of the supporting structure, save engineering materials, and ensure the safety and stability of the construction. Due to anchoring technology of cable has many advantages such as active support, safety and economy, it has been widely used in railway engineering, slope engineering and water conservancy engineering for landslide management and high slope support in the world [1].

Since the middle of the 1960s, anchor cables were used in Australian mines for the first time to strengthen the rock mass. After more than 30 years of development, from the structure of the anchor cable, manufacturing and quality, supporting construction equipment, anchoring mechanism, parameter design methods, application scope and other aspects have been rapidly developed and improved [2]. For the anchoring mechanism of the anchor cable is very complex, there isn't a proper calculated model for the engineering design of the anchor cable till now [3]. Because the anchor cable is a space spiral structure, when the anchor cable is pulled, a reverse torque is often generated, which can reduce the axial tension of the cable. Not considering the torque effect has a great impact on the evaluation of the carrying capacity of the anchor cable, so the design theory without the torque effect of the anchor cable can not meet the needs of engineering practice [4].

There isn't a proper calculated model for the anchor cable, the design theory of anchor cable can not meet the needs of engi-

neering practice. Therefore, it is important to reveal the coupling effect of anchor cable tension and reverse torque in the axial tensile tests and propose a reasonable calculation model, which is of great theoretical significance and practical value for deepening the anchoring mechanism of the anchor cables.

2. STATE OF THE ART

In the past years, with the increasing application of anchor cables, its mechanical properties have gradually attracted people's attention. Kang et al. divided the axial load-displacement curve of the stranded wire into four stages through the pull-out tests: the initial loading stage, the elastic deformation to yield stage, the post-yield strengthening stage, and the breaking stage [5]. Zhang et al. developed a method for detecting the broken wire of a steel strand under axial tension and fitted a linear formula of the axial force and the strain [6]. Kong et al. theoretically derived the elastic modulus of the steel strand and performed finite element analysis on the steel strand. They found that it is not appropriate to use an equal-section round rod to equivalent steel strand under complex stress conditions. However, they did not explain how the elastic modulus of the steel strand develop in a complex stress state [7]. Ghoreishi et al. compared the existing theoretical model of steel strand with the finite element model and they found that when the twist angle is greater than 20°, the theoretical model is not accurate for the calculation of the axial elastic stiffness [8]. Chen and Yuan carried out the finite element simulation of the friction influence on the section stress of the stranded wire, but they only analyzed the section stress of the stranded wire in the elastic stage [9]. Wu et al. performed a finite element analysis on the stress distribution and failure mode of the steel strand [10]. These studies have revealed the mechanical response of the steel strands under axial loading, but ignored the torque effect of the steel strands.

Recently, there are lots of studies about the steel wire ropes. The structure of the steel wire rope is similar to the steel strand. However, the flexibility of the steel wire rope is better than that of the steel strand, and the main function of the steel wire rope is tension, which does not consider the problem of looseness. While its research experience can be used for a reference to the steel strand. Costello proposed a nonlinear analytical model for predicting the mechanical properties of single-stranded steel wire ropes. However, this model only considered the influence of Poisson's ratio and ignored the contact deformation of the wires and the plasticity of materials [11]. Utting & Jones proved that the internal friction and contact deformation had little effect on the steel wire rope, but which had the large effect on the deformation of each individual wire [12]. Jiang et al. studied the indefinite contact static problem of a single-stranded 1 × 7 steel wire rope under the rigid fixed constraint at the end by using the finite element method, they found that the radial and lateral contact occured simultaneously under the axial tensile load [13]. Beltran & Vico analyzed the static properties and stress-strain distribution in the cross-section of a steel wire rope with asymmetric failure [14]. Yu et al. researched the mechanical properties and wire-to-wire stress state of the steel wire rope under the transverse loading [15]. Nikolaos & Gerald analyzed the axial and torsional responses of spirals and their internal coupling from the perspective of the mechanical analysis and numerical simulation, but no experimental verification was performed [16]. Chen et al. compared and analyzed the overall mechanical characteristics and the contact stress of simple round rope strands and the spiral triangle strands with the same structural parameters under the axial and torsion loading [17]. Xing and Zhou studied the relationship between the bending moment and the curvature of the 1 × 7 strands by directly applying the bending moment at the loading end [18]. Zhang et al. studied the dynamic torsion characteristics and the internal spiral state of steel wire ropes by using the theoretical analysis model, but the model was only suitable for the elastic phase [19]. Cao & Wu proposed a new bending mechanical modeling method for the steel wire ropes [20]. These studies mainly focused on the theoretical derivation and numerical simulation, but there is few experiments have been performed to verify the axial mechanical response of the anchor rope under free rotation conditions, and few reports have quantitatively analyzed the coupling effect of tension and torsion of the anchor cable.

In view of the shortcomings of the existing studies, this study used a new type equipment self-developed to measure the relationship between the axial tension and torque, and conducted the axial tensile tests under the condition including the anchor cable with no rotating and rotating freely. Then the decoupling study of the axial loading and the reverse torque was performed. The anchoring effect of rock and soil is closely related to the mechanical properties of the anchor cable component. To reveal the coupling mechanism of the axial loading and the reverse torque of the anchor cable is of great significance for the type selection, structural design and operating maintenance of the anchor cable.

The remainder of this study is organized as follows. The third part describes the experimental design and finite element modeling. The fourth part analyzes the experimental data and numerical test. The last part summarizes this article and gives the relevant conclusions.

3. METHODOLOGY

3.1. MATERIALS AND LOADING SCHEME

3.1.1. Materials and test plan

The test anchor cables 1 × 7 steel strand was produced by Tianjin Ruitong Limited Company, which was made of high carbon steel wire rod through cold drawing and twisting. These anchor cables had three diameters (9.5 mm, 12.7 mm, 15.2 mm), and each diameter was divided into three lengths (850 mm, 1150 mm, 1350 mm). These anchor cables were used for the axial tensile experiments with different locking lengths. The specification parameters of anchor cables with different diameters are shown in Table I.

By changing the diameter of the anchor cable, rotation conditions and locking length, the influence of each factor on the peak tension, peak torque, and the axial force-displacement curve of the anchor cable was investigated. The experimental scheme is shown in Table II, where NR means no rotation and R means free

Structure	Nominal diameter (mm)	Cross-section area (mm^2)	Strength level (MPa)	Maximum load (kN)	Measured twist distance (mm)	Unit weight (kg/km)
1×7 Standard type	9.5	54.8	1860	102	150	430
	12.7	98.7	1860	184	200	775
	15.2	140	1860	260	210	1101

Table I: Main parameters of the anchor cables

Sample type	Diameter (mm)	Locking length (mm)
NR9 (D1, D2, D3)	9.5	500, 750, 1000
NR12 (D1, D2, D3)	12.7	
NR15 (D1, D2, D3)	15.2	
R9 (D1, D2, D3)	9.5	
R12 (D1, D2, D3)	12.7	
R15 (D1, D2, D3)	15.2	

Table II: Test plan of the anchor cables

rotation conditions, D1, D2, and D3 represent the locking lengths of 500, 750, and 1000 mm, respectively. In order to eliminate the influence of error, each group of the axial tensile experiments was repeated three times, and the experimental data were averaged, with a total of 54 in 18 groups. Before the test, the supporting anchors were installed at both ends of each anchor cable, and the upper anchor is 50 mm away from the top to prevent early failure due to excessive sliding of the anchor. Some anchor cables of the samples are shown in Fig. 1.

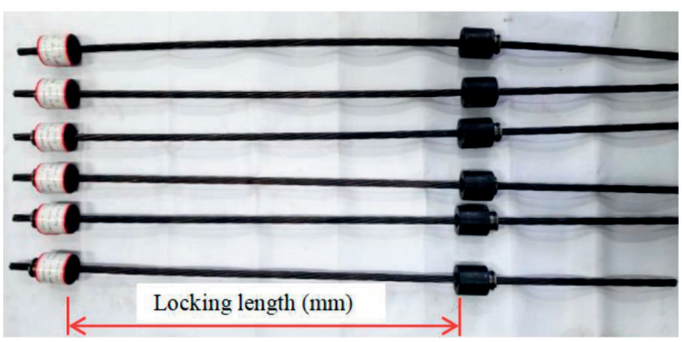


Fig. 1: Test samples of the anchor cables

3.1.2. Test device and loading scheme

The LW-1000 self-developed equipment was adopted for the torque and axial force of the anchor cable during the test, which was composed of loading device, measuring device, data acquisition and processing system (Fig. 2). This equipment can realize the functions of real-time collection of test data, timely displaying and real-time drawing of charts and so on. The technical parameters of the device were shown in Table III.

As shown in Fig. 2(b), the technical solution is that a lower beam 1 is installed between the cylinders of the oil cylinders on both sides, and the upper beam 2 is fixed between the piston rods of the oil cylinders on both sides. The upper beam is provided with a rotating stretching and rotating tension shaft 3, and the lower end of the stretching and rotating tension shaft is provided with an anchor cable 9. A torque sensor 7 is installed on the beam, and the torque sensor 7 and the upper end of the tension rotation tension shaft 3 are connected by a swing rod 6 to constitute a torque test structure of the anchor cable. The upper end of the piston rod of the oil cylinder is fixed to the upper beam through a transitional pusher 4. A load sensor 5 is provided between the transitional pusher and the upper cross-beam. A positioning gauge is provided to limit the relative rotation of the tensile rotation shaft and the upper cross-beam Pin 8. The device can carry out the axial tensile test of the anchor cable under no rotation and free rotation and conditions.

The axial tensile test of the anchor cable adopts the test method of China Standard GB/T 228-2002 for metal materials at room temperature. The anchor cable sample is installed in the fixture of the testing machine according to the set length, the upper end of the steel strand controls whether it rotates freely and the lower end is fixed. This testing takes the equal loading force control, the loading speed is 1.0 kN/s, until the strand is broken, and timely recording the load-displacement curve of the anchor cable.

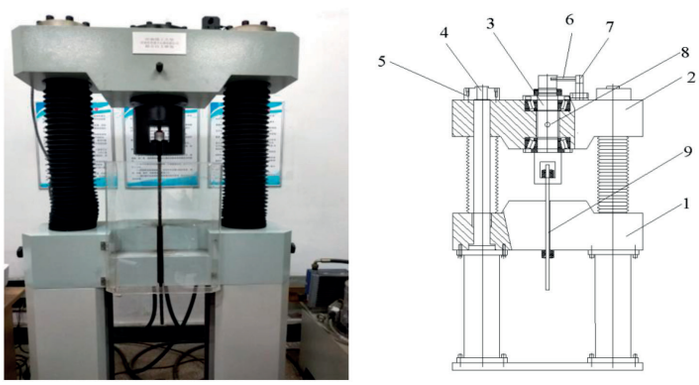
3.2. NUMERICAL SIMULATION ANALYSIS

3.2.1. Computational model and its parameters

As shown in Fig. 3, the three-dimension model was built by using ABAQUS. In view of the geometric characteristics and contact factors of the steel wire, the 8-node cuboid unit C3D8R with reduced integration and hourglass control was used to mesh the steel strand by the sweep method, which could prevent the locking occurrence. To balance the calculation efficiency and calculation accuracy, a single steel wire was taken for analysis of 32 and 500 elements in the radial and axial directions, which generated 144033 nodes and 112192 elements. The material parameters of the computational model were set as follows: elastic modulus E 80 GPa, Poisson's ratio ν 0.3, yield stress 1790 MPa, tensile strength 1950 MPa, and yield strain 5%.

3.2.2 Boundary conditions and loading process

In order to simulate the restraint effect of the fixture on the anchor cable, the degrees of freedom of the node on the end face

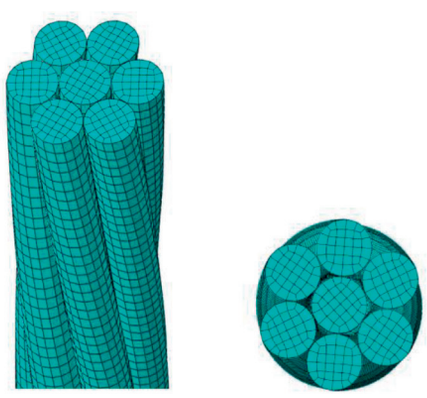


(a) (b)

Fig. 2. The loading and measurement device. (a) Test equipment diagram; (b) Structural diagram

Tension (kN)	Torque (N·m)	Displacement (mm)	Rate of loading (kN/s)	Rate of displacement (mm/min)
0-1000	0-500	0-1100	0.01-5.00	0.05-500

Table III: The technical parameters of the device



(a) (b)

Fig.3: Computational model and its meshes of cable-bolts. (a) Computational model; (b) Cross-section of the model

of the anchor cable are coupled with the reference point by means of kinematic coupling, where one end is fully constrained, the other five degrees of freedom except axial movement are zero when the other end is not rotated, and the other four degrees of freedom except axial movement and rotation are zero in the rotating case (Fig. 4 (See section: supplementary material)). The general contact method is adopted, the normal contact property among the adjacent steel wires is set to hard contact. The tangential contact property uses general friction and the friction coefficient is set to 0.15. Since the nonlinear factor of the anchor cable is not easy to converge by static algorithm, the mechanical characteristics of anchor cable are simulated by ABAQUS/Explicit simulation quasi-static method. The displacement loading method is adopted, and the smooth analysis step loading is used along the axial direction of the anchor cable, and the stretching distance is 40 mm.

4. RESULT ANALYSIS AND DISCUSSION

4.1. FAILURE CHARACTERISTICS ANALYSIS

The typical failure forms of these anchor cables are shown in Fig. 5 (See section: supplementary material). It can be found that the breakage of the anchor cable was accompanied by the untwisting behaviour, and there were obvious sliding traces among these steel wires. The peripheral steel wire near the clamp was first pulled off, and the other end of the anchor cable was exploded near the clamp. The neck fractures occurred in the steel wires, and most of the fractures were cup-cone-shaped fractures, and a few of that are split fractures.

In addition, it was found that the whole process of the axial tensile test did not change significantly under the condition of non-rotation, and the rebound deformation occurred at the moment when the steel wire was broken. Under the condition of free rotation, the anchor cable would twist in the loosening direction., it stopped after twisting a certain angle until it was pulled off. The final breaking result is similar to that of the condition of not rotation.

4.2. SENSITIVE INFLUENCING FACTORS ANALYSIS

According to the experimental data, the graphs of the peak tension and peak torque under different factors are shown in Fig. 6 (See section: supplementary material). The torque was measured under non-rotating condition and the torque was zero under free-rotating condition. The average value of the test data of each group anchor cables was taken.

It can be found from Fig. 6 (See section: supplementary material), there are no obvious differences between these peak tensions of the anchor cables under the condition of rotation and no rotation, and both increase with the increase of the diameter. Compared with the 9.5 mm diameter cable, the peak tension of the 12.7 and 15.2 mm diameter anchor cable increases 1.8 and 2.5 times, respectively. The peak tension remains the same as the locking length of the anchor increases, namely the peak tension remains basically unchanged with the increase of the locking length.

The peak torque also increases with the increase of the anchor cable diameter without rotation. Compared with the 9.5 mm diameter cable, the peak torque of the 12.7 and 15.2 mm diameter anchor cable increases 5 and 10 times, respectively. The peak torque remains the same as the locking length of the anchor increases. These results show that the diameter of anchor cable has a great effect on the peak tension and peak torque, while the locking length has little effect on that values of the anchor cable.

4.3. TENSION-DISPLACEMENT-TORQUE CURVES ANALYSIS

Since the locking length has little effect on the torque and tension, the typical axial force-displacement-torque curves of anchor cables with different diameters at a locking length of 500 mm are shown in Fig. 7. The displacement in Fig. 7 includes not only the tensile displacement of the steel strand, but also the sliding displacement between the steel strand and the clamp.

It can be found from Fig. 7, the axial force-displacement-torque curves of the anchor cables display three stages:

Stage 1 (pre-tensioning stage): In the initial stage of loading, the tension of the anchor cable increases gradually and the torque is basically zero.

Stage 2 (elastic stage): the torque of the anchor cable starts to increase, and increases linearly with the increase of the tensile force, until the anchor cable yields.

Stage 3 (plasticity stage): the axial force of the anchor cable is increased slightly and the torque of the anchor cable is basically stable until eventually destroyed.

As shown in Fig. 8 (See section: supplementary material), the torque change of the anchor cable in tension can be divided into elastic and plastic stages, and the change law of torque in different stages is very different.

Based on the experimental data, the empirical formula for torque of anchor cable is fitted, and the torque expressions of anchor cables with different diameters are as follows:

$$M = cP\mathrm{d} = \left(0.025 + 7.045\times10^{-5} e^{0.318d}\right)Pd \tag{1}$$

where, M is the torque of anchor cable, N·m; P is the axial force of anchor cable, kN; c is the torque coefficient, and d is the anchor diameter, mm, R^2=0.99.

4.4. AXIAL TENSILE FORCE DECOUPLING ANALYSIS

The typical axial force-displacement curves of different diameter anchor cables under rotation and non-rotation conditions are shown in Fig. 9 (See section: supplementary material).

Comparing the axial force-displacement curves of three diameter anchor cables under different rotation conditions, it can be found that the elastic modulus of the anchor cable will decrease under free rotation. After entering the plastic stage, the tensile force increases faster than that of the the non-rotation condition, but the peak tension is basically the same. Since the torque of the anchor cable is released under free rotation condition, part of the work done by pulling force is used to reverse, ignoring friction and other factors. The work induced by rotation of the anchor cable is equivalent to that of the reverse rotation force ΔF in tensile displacement. According to the work-energy principle:

$$W_1 - W_2 = \frac{\Delta FS}{2} \tag{2}$$

According to Eq. (2), the tension-torque coupling formula is proposed as follows:

$$\eta = \frac{\Delta F}{F} = \frac{2(W_1 - W_2)}{FS} \tag{3}$$

where, W_1 is the work of the anchor cable performed under free rotation condition, J. W_2 is the work of the anchor cable performed under non-rotating condition, J. The work can be obtained by integrating the axial force-displacement curve. ΔF is the reverse rotation force, kN, and S is the displacement, mm. η is the axial force-torque coupling coefficient, which is the percentage of the reverse rotation force used for untwisting to the total axial

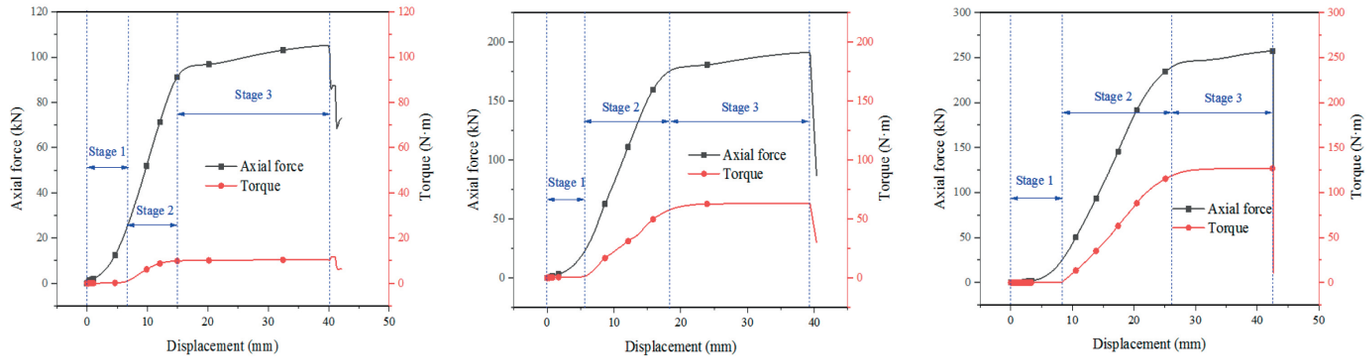


Fig. 7: Axial force-displacement-torque curves of different diameter cables. (a) 9.5 mm anchor cable; (b) 12.7 mm anchor cable; (c) 15.2 mm anchor cable

force. Calculated according to Fig. 9 (See section: supplementary material), the ratios of the tensile-torque coupling coefficients for the three diameters of the anchor cables are 11%, 12%, and 10%, respectively.

It can be seen from Fig. 10, in general, the axial force-displacement curves obtained by the tests and numerical analysis match well, but the displacement of the elastic phase is not consistent. The main reason for this is that the experiment has a pretension stage, so there is nonlinear loading in the early stage, while the simulation is linear loading. However, the regularity of rotation and non-rotation remain the same, both stiffness decreases under free rotation condition. The peak tension tends to be almost the same, and the torque coefficients are in good agreement (Fig. 13 (See section: supplementary material)).

4.5. DISCUSSION

As shown in Fig. 11 (See section: supplementary material), since anchor cable is made by twisting 6 outer steel wires around 1 core steel wire, the outer steel wire is a single twisted steel wire. When the anchor cable is axial pulled, there are internal forces among these steel wires, which can be decomposed into the axial force parallel to the axis of the anchor cable and the horizontal force perpendicular to the axis of the anchor cable, which will reverse the torsion of the anchor cable. Ignoring the friction among these steel wires, the force of the steel wire meets the following relationship:

$$F = F_0 + F_1 \tag{4}$$

$$M = nTR\cos\alpha \tag{5}$$

where, F is the total axial force of the anchor cable. F_0 is the axial force of the inner wire. F_1 is the tensile component of the outer wire along the axial direction of the anchor cable. M is torque of the anchor cable. n is the number of outer wires, T is the axial force of the outer wire, and R is the spiral radius. Assuming that the radius of the inner and outer wire is equal, then $R = r_0 + r_1 = 2r_1$. α is the helix angle, which is the angle between the tangent of the outer wire helix and the inner wire.

Select a helical steel wire within a twist range and expand it around the inner wire as shown in Fig. 12 (See section: supplementary material). The inner and outer wires of the anchor cable satisfy the triangular relationship, where P is the twist distance (the length of the anchor cable corresponding to the 360° rotation of the helical wire), L is the length of the outer helix. The twisted shape of the spiral wire under the axial load of the anchor cable will change. After its deformation, the strain relationship between the inner and outer wires of the anchor cable can be expressed as [11]:

$$\varepsilon_1 = \frac{L_2 - L}{L} = (1+\varepsilon_0)\frac{\sin\alpha}{\sin\alpha_2} - 1 \tag{6}$$

where, ε_1 is the strain of the outer wire, ε_0 is the strain of the inner wire, and P_2, L_2, α_2, and R_2 are the twist length, helix length, helix angle, and helix radius after deformation.

Considering the influence of Poisson's ratio, the helix radius after loading changes to:

$$R_2 = r_0(1-\nu\varepsilon_0) + r_1(1-\nu\varepsilon_1) \tag{7}$$

Then the helix angle before and after deformation satisfies the following relationship.

$$\tan\alpha_2 = \frac{P(1+\varepsilon_0)}{2\pi R_2} = \tan\alpha\frac{2(1+\varepsilon_0)}{2-\nu(\varepsilon_0+\varepsilon_1)} \tag{8}$$

According to the law of elasticity:

$$(\varepsilon_0 + n\varepsilon_1\sin\alpha_2)\ EA = F \tag{9}$$

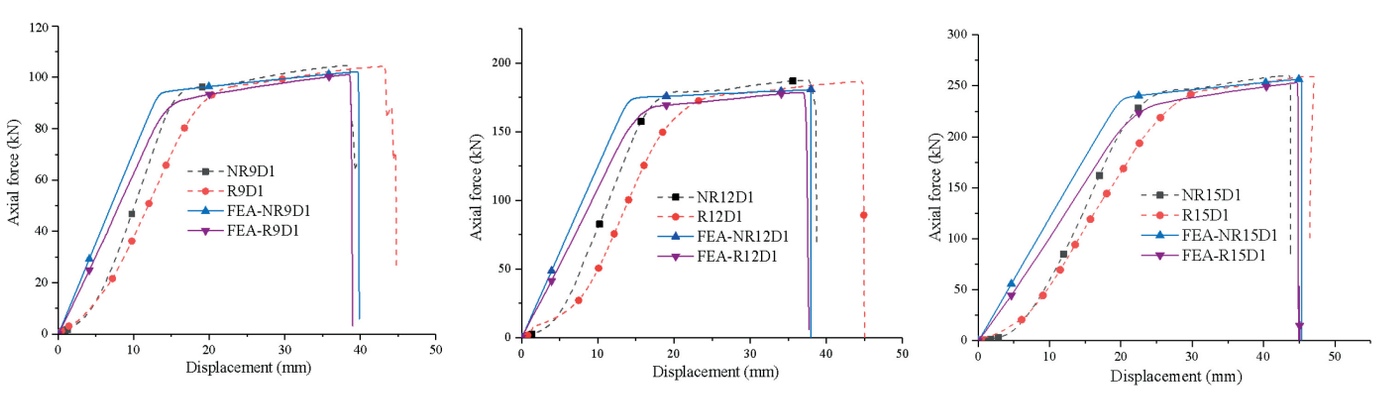


Fig. 10: Comparison between the calculation and experimental results. (a) 9.5 mm anchor cable; (b) 12.7 mm anchor cable; (c) 15.2 mm anchor cable

$$n\cos\alpha_2 EA\ \varepsilon_1 R_2 = M \tag{10}$$

Substituting Eqs. (6) to (8) into Eq. (9), then Eq. (10) can find the relationship between *F* and *M*. where, *E* is the elastic modulus and *A* is the cross-sectional area of the steel wire. Compare the analytical results with the experimental results, as shown in Fig. 13 (See section: supplementary material).

As shown in Fig. 13 (See section: supplementary material), the torque coefficient obtained by the theory is basically consistent with the test, but it is slightly larger, because the formula is mainly simplified and the influence of friction and bending moment are ignored. Eq. (10) is the axial force-torque relationship under non-rotating condition. The change of helix angle is very small and it can be negligible. If allowing the the anchor cable rotate freely, the torque the anchor cable is released, and the outer wire is turned in the loose twist direction, the helix angle changes greatly. According to Eq. (6), the strain of the outer wire decreases under the same displacement, so the elastic modulus will decrease.

5. CONCLUSIONS

To study the axial force-torque coupling effects and mechanical properties of the anchor cable, a new type of self-developed equipment was used to perform the axial force test of the anchor cable. Based on the tests, the axial force-torque coupling effect is analyzed, and the results are verified by the numerical simulation. The main conclusions are obtained as follows.

(1) The peak tension and peak torque both increase with the diameter of the anchor cable. Compared with the 9.5 mm diameter cable, the peak tension of the 12.7 and 15.2 mm diameter anchor cable increases 1.8 and 2.5 times, respectively. The peak torque increasing has the similarly characteristics with the increase of the diameter of the anchor cable. While the effect of the locking length on the peak tension and torque is not obvious.

(2) The reverse torque generated by the anchor cable being pulled under no rotate condition is divided into the elastic and plastic phases. The torque in the elastic phase increases linearly with the increase of the tensile force. When the steel strand reaches the yield strength, the torque is basically stable and the tensile force increases slightly. According to the experimental tension-torque curve, a torque empirical formula of anchor cables with different diameters is fitted.

(3) Under the condition of free rotation, the elastic modulus of the anchor cable will be reduced, and the peak tensile force of rotation and non-rotation is basically the same. Based on the work and energy principle, a tension-torsion coupling formula is proposed, the percentage of the axial tension force used for untwisting of the cables with three different diameters (9.5 mm, 12.7 mm, 15.2 mm) are 11%, 12%, and 10%, respectively.

In a word, this study revealed the decoupling of axial force and torque by means of the axial tensile experiments and numerical simulations, obtained the coupling coefficients of the axial force and torque of the anchor cables with different diameters, fitted the empirical formulas of the torque of anchor cables of the anchor cables with different diameters, and provide theoretical basis and technical support for engineering practice. In the next work, the failure mechanism of the anchorage segment induced by the untwisting of the anchor cable needs to be further studied.

REFERENCES

[1] He SM, Wang QC. "Problems of the Study on Mechanism of Anchor Cable". Chinese Journal of Underground Space and Engineering. January 2006. Vol. 2-1. p. 160-165. DOI: 10.3969/j.issn.1673-0836.2006.01.036
[2] Wang SR, Xiao HG, Hagan P, Zou ZS. "Mechanical behavior of fully-grouted bolt in jointed rocks subjected to double shear tests". DYNA, March 2017. Vol. 92-3. p. 314-320. DOI: http://dx.doi.org/10.6036/8325
[3] Liu XR, Liu YQ, Kang JW, Yang ZP. "Prestress loss laws of anchor cables in foundation pits and control measures of tension by steps". Chinese Journal of Geotechnical Engineering. October 2015. Vol. 37-10. p.1794-1801. DOI: 10.11779/CJGE201510007
[4] Bawden WF, Hyett AJ, Lausch P. "An experimental procedure for the in situtesting of cable bolts". International journal of rock mechanics and mining sciences & geomechanics abstracts. September 1992. Vol. 29-5. p. 525-533. DOI: 10.1016/0148-9062(92)92635-P
[5] Kang HP, Yang JH, Jiang PF. "Tests and analysis on mechanical properties for cable bolts". Coal Science and Technology. June 2015. Vol. 43-6. p. 29-33. DOI: 10.13199/j.cnki.cst.2015.06.006
[6] Zhang XP, Wang XL, Xing HN, Li D. "Experimental research on mechanical properties of prestressing steel strand". Metal Products. March 2016. Vol. 42-3. p. 1-5. DOI: 10.3969/j.issn.1003-4226.2016.03.001
[7] Kong QK, Wan P. "Basic mechanical properties and finite element method simulation of steel strand." Engineering Structure. 2003. Vol. 23-1. p. 20-22. DOI:10.3969/j.issn.1007-8983.2003.01.010.
[8] Ghoreishi SR, Messager T, Cartraud P, Davies P. "Validity and limitations of linear analytical models for steel wire strands under axial loading, using a 3D FE model". International Journal of Mechanical Sciences. November 2007. Vol. 49-11. p. 1251-1261. DOI: 10.3969/j.issn.1007-8983.2003.01.010
[9] Chen C, Yuan FX. "Fine analysis of section stress of steel strand". Journal of Zhejiang University(Engineering Science). May 2017. Vol. 51-5. p. 841-846. DOI: 10.3785/j.issn.1008-973X.2017.05.001
[10] Wu ZJ, Ding Z, Sun CP, Zhang LM. "Finite element analysis of section stress and failure mode of steel strand". China science paper. June 2019. Vol. 13-22. p. 2623-2628. DOI: 10.3785/j.issn.1008-973X.2017.05.001
[11] Costello GA. Theory of wire rope (2nd ed). New York: Springer, 1997. ISBN 978-1-4621-1970-5. DOI: 10.1007/978-1-4612-1970-5
[12] Utting WS, Jones N. "The response of wire rope strands to axial tensile loads-Part 11 comparison of experimental results and theoretical predictions". International Journal of Mechanical Science. January 1987. Vol. 29-9. p. 621-636. DOI: 10.1016/0020-7403(87)90033-6
[13] Jiang WG, Warby MK, Henshall JL. "Statically Indeterminate Contacts in Axially Loaded Wire Strand". European Journal of Mechanics A/Solids. January-February 2008. Vol. 27-1. p. 69-78. DOI: 10.1016/j.euromechsol.2007.02.003
[14] Beltran JF, Vico ED. "Assessment of static rope behavior with asymmetric damage distribution". Engineering Structures. March 2015. Vol. 86. p. 84-98. DOI: 10.1016/j.engstruct.2014.12.026
[15] Yu YJ, Chen ZH, Liu HB, Wang XD. "Finite element study of behavior and interface force conditions of seven-wire strand under axial and lateral loading". Construction and Building Materials. September 2014. Vol. 66. p. 10-18. DOI: https://doi.org/10.1016/j.conbuildmat.2014.05.009
[16] Nikolaos K, Gerald K. "Mechanical response of a helical body to axial, torsional and radial strain". International Journal of Mechanical Sciences. May 2015. Vol. 94–95. p. 260-265. DOI: 10.1016/j.ijmecsci.2015.02.022
[17] Chen YP, Meng FM, Gong XS. "Parametric modeling and comparative finite element analysis of spiral triangular strand and simple straight strand". Advances in Engineering Software. October 2015. Vol. 90. p. 63-75. DOI: https://doi.org/10.1016/j.advengsoft.2015.06.011
[18] Xing EZ, Zhou CY. "Analysis of the bending behavior of a cable structure under microgravity". International Journal of Mechanical Sciences. August 2016. Vol. 114. p. 132-140. DOI: https://doi.org/10.1016/j.ijmecsci.2016.05.013
[19] Zhang J, Wang DG, Zhang DK, et al. "Dynamic torsional characteristics of mine hoisting rope and its internal spiral components". Tribology International. May 2017. Vol. 109. p. 182-191. DOI: https://doi.org/10.1016/j.triboint.2016.12.037
[20] Cao X, Wu WG. "The establishment of a mechanics model of multi-strand wire rope subjected to bending load with finite element simulation and experimental verification". International Journal of Mechanical Sciences. July 2018. Vol. 142-143. p. 289-303. DOI: https://doi.org/10.1016/j.ijmecsci.2018.04.051.

ACKNOWLEDGEMENTS

This work was financially supported by the National Natural Science Foundation of China (51774112; 51674190), the International Cooperation Project of Henan Science and Technology Department (182102410060), the Doctoral Fund of Henan Polytechnic University (B2015-67).

SUPPLEMENTARY MATERIAL

https://www.revistadyna.com/documentos/pdfs/_adic/9603-1.pdf